Recent results from heavy ion collisions at LHCb

O. Boente García⋆ on behalf of the LHCb collaboration

Instituto Galego de Física de Altas Enerxías (IGFAE, USC)

⋆ oscar.boente@usc.es

Abstract

LHCb is a fully instrumented spectrometer covering the forward rapidity region at the LHC, which provides unique access to the small Bjorken-x region inside the nucleus. In this contribution, a selection of recent results from the LHCb heavy-ion program are presented, including a measurement of charged hadron production in proton-proton (pp) and proton-lead (pPb) collisions, χ_{c2}/χ_{c1} production in pPb collisions, and coherent J/ψ production in peripheral and ultra-peripheral PbPb collisions. Comparisons with calculations and effects from the nuclear PDFs and dense QCD medium are discussed.

1 Introduction

The LHCb experiment [1,2], located at the Large Hadron Collider (LHC) at CERN, is a forward spectrometer fully instrumented between 2 and 5 units of pseudorapidity (η), thus covering an acceptance not accessible by the other LHC experiments. The detector consists of a silicon-strip vertex detector (VELO) surrounding the interaction region to determine the position of the collision point (primary vertex) and the decay vertices of B and D hadrons, a tracking system that provides a measurement of the momentum, p, of charged particles, two ring-imaging Cherenkov detectors for charged hadron discrimination, calorimetry and a muon system.

LHCb has participated in most heavy-ion data-taking campaigns at LHC and so far has collected data from proton-lead collisions (pPb) at centre-of-mass energy of $\sqrt{s_{\mathrm{NN}}} = 5.02$ and 8.16 TeV and lead-lead (PbPb) collisions at $\sqrt{s_{\mathrm{NN}}} = 5.02$ TeV. When acquiring pPb data the directions of the proton and lead beams are switched so that the *forward* region, with the proton going towards the LHCb spectrometer ($\eta > 0$), and the *backward* region, with the lead going towards the LHCb spectrometer ($\eta < 0$), can be accessed. These datasets allow for measurements to characterise cold nuclear matter effects and the dense QCD medium, such as those presented in these Proceedings.
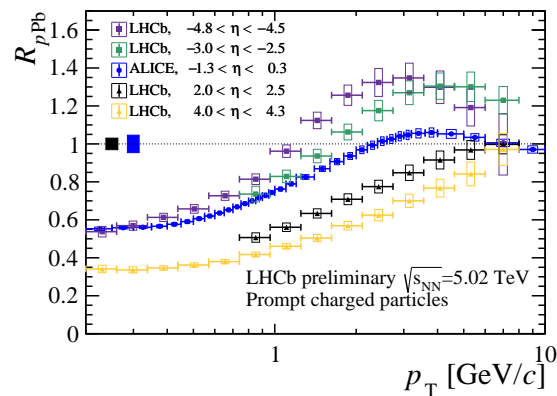
Figure 1: Right: Nuclear modification factor measured as a function of p_T by the LHCb [3] and the ALICE collaborations [4] at $\sqrt{s_{NN}} = 5.02$ TeV. Vertical error bars account for statistical uncertainty, open boxes for uncorrelated systematic uncertainty. The correlated uncertainty from the normalisation is indicated with a filled black (blue) box at $R_{pPb} = 1$ for LHCb (ALICE).

2 Prompt charged particle production in pPb and pp collisions at 5.02 TeV

The production of prompt charged particles is studied in pPb and pp collisions at the centre-of-mass energy $\sqrt{s_{NN}} = 5.02$ TeV with respect to their pseudorapidity (η) and transverse momentum (p_T) [3]. Double-differential production cross-sections are obtained for particles with $p > 2$ GeV/c, $0.2 < p_T < 8.0$ and different η coverage depending on the beam configuration: $2.0 < \eta < 4.8$ for pp, $1.5 < \eta < 4.3$ for pPb (forward) and $-2.5 < \eta < -5.2$ for pPb (backward). Prompt charged particles and their momentum are measured with the LHCb tracking system. Raw track yields need to be corrected with reconstruction and selection efficiencies. Additionally, background contributions originating from fake tracks not corresponding to real particles and non-prompt particles are determined to correct the yields. For most (η, p_T) intervals, the total uncertainty of pp and pPb production cross-sections is around 3%.

The measured cross-sections allow the nuclear modification factor $R_{pPb} \equiv \sigma_{pPb}/(A\sigma_{pp})$ for charged particles to be computed for the first time in the forward and backward regions at the LHC. The R_{pPb} result is shown in Fig. 1. In the forward region, R_{pPb} shows a suppression of charged particle production, in general agreement with expectations from nuclear PDFs [5] and saturation models [6]. In the backward region, an enhancement of charged hadron production is seen for $p_T > 1.5$ GeV/c. This feature is not well described by nuclear PDFs [5] or by a pQCD calculation considering parton multiple scattering [7], which reproduced the enhancement observed by the PHENIX collaboration in the backward region of proton-gold collisions [8]. In Fig. 1, the LHCb result is compared with the ALICE result in the central η region [4], showing the continuity of the R_{pPb} trend. The measurement places stringent constraints to the nuclear PDFs and saturation models down to very low x for values around 10^{-6} with a total relative uncertainty in the R_{pPb} determination down to 4.2%.
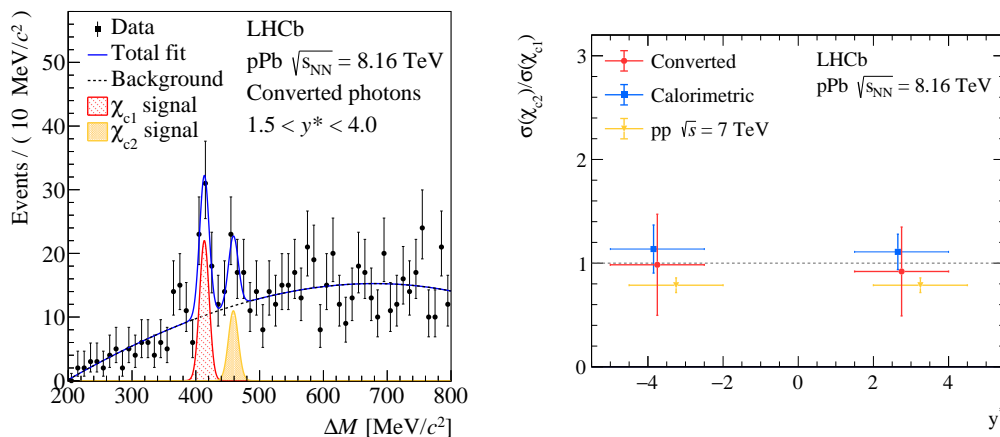
Figure 2: Left: mass-difference spectrum of converted χ_{c1} and χ_{c2} candidates in the forward configuration data, superimposed with a fit to χ_{c1} and χ_{c2} signals and combinatorial background. Right: cross-section ratio, $\sigma(\chi_{c2})/\sigma(\chi_{c1})$ as a function of centre-of-mass rapidity y^*, in pPb [9] at 8.16 TeV and pp collisions at $\sqrt{s} = 7$ TeV [10].

3   Prompt-production cross-section ratio χ_{c2}/χ_{c1} in pPb collisions

The LHCb experiment has measured the ratio of the production cross-sections of χ_{c2} and χ_{c1} quarkonium states in pPb collisions for the first time at LHC [9]. The study relies on data from collisions at $\sqrt{s_{NN}} = 8.16$ TeV in the forward and backward configurations with a integrated luminosity of $14\,\mu b^{-1}$ and $21\,\mu b^{-1}$, respectively. Candidates of χ_{c2}, χ_{c1} mesons are identified using the radiative decay $\chi_c \rightarrow J/\psi(\rightarrow \mu^+\mu^-)\gamma$. The J/ψ meson is identified by its decay into two muons, and the distance between the dimuon vertex and the primary vertex is used to select exclusively prompt candidates. The photon is detected with two independent techniques: directly from signals in the electromagnetic calorimeter, and detecting electrons from photon conversions within the detector material. The latter provides a better mass resolution but poor statistics, as seen in Fig. 2 (left).

The measurement of the χ_{c2} and χ_{c1} cross-sections ratio benefits from the cancellation of efficiencies similarly affecting both states, since they have very close decay kinematics. The result of this ratio in the forward and backward regions for both γ detection strategies is presented in Fig. 2 (right). The ratio is compatible with unity showing no rapidity dependence, and is compatible within uncertainties with the pp collisions ratio at 7 TeV [10]. This indicates that nuclear effects have a similar impact on both states, within uncertainties.

4   Coherent J/ψ production in ultra-peripheral and peripheral PbPb collisions

LHCb has measured the production of coherent J/ψ from data of ultra-peripheral PbPb collisions taken in 2015 with an integrated luminosity of $\mathcal{L} = 10.1 \pm 1.3\,\mu b^{-1}$ [11]. Candidates for J/ψ are selected by requiring no significant activity in the calorimeters and the HeRSCheL counters [12], which indicates the presence of rapidity gaps. The J/ψ signal is extracted with a fit to the dimuon mass distribution, and then the yield of coherently produced J/ψ is obtained
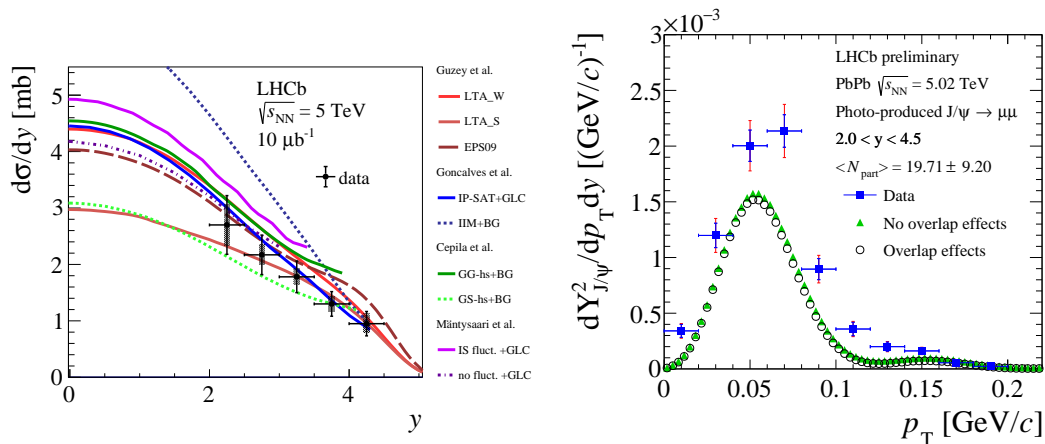
Figure 3: Left: differential cross-section as a function of rapidity for coherent J/ψ production compared to different phenomenological predictions [11]. Right: double-differential yields of photo-produced J/ψ candidates as a function of p_T. In both figures, the inner bars represent the statistical uncertainty while the outer bars show the total uncertainty.

with a template fit to the $\log(p_T^2)$ distribution that includes contributions from coherent and incoherent J/ψ production, non-resonant background and feed-down from $\psi(2S) \rightarrow J/\psi \pi^+ \pi^-$ decays. The result of the cross-section with respect to the rapidity is shown in Fig. 3 (left), where the result is overlaid with several phenomenological predictions (see [11] for details).

Additionally, the production of coherent J/ψ can be studied in peripheral PbPb collisions. Photo-produced J/ψ mesons, which distinctively have low average p_T, are a possible explanation for the enhancement of R_{AA} for J/ψ mesons at low p_T previously observed by other experiments in peripheral ion-ion collisions [13,14]. LHCb has studied this system with data of PbPb collisions taken in 2018 corresponding to an integrated luminosity about 210 μb^{-1}. The J/ψ signal is extracted with a fit to the dimuon mass and then the contribution of coherent J/ψ is separated from the hadro-produced J/ψ with a fit to the $\log(p_T^2)$ distribution. The resulting coherent J/ψ yields are corrected for detection efficiencies and are studied with respect to p_T, y and the centrality of the collisions, which is determined by the energy collected in the electromagnetic calorimeter. Fig. 3 (right) shows the p_T distribution of coherently produced J/ψ, determined precisely for the first time. The measured distribution is compared with a phenomenological prediction [15].

5 Conclusions and outlook

The presented measurements demonstrate the unique capabilities of LHCb for the study of strongly interacting matter and nuclear effects in different systems. For the upcoming LHC Run 3, important increases of the data sample sizes of pPb and PbPb events are expected, which will improve the current precision and will make new analyses possible. The centrality reach in PbPb, currently limited to around 60% most central collisions, is foreseen to increase up to 30% most central collisions, opening new horizons to study deconfined matter in this system.

References

[1] A. A. Alves Jr. et al., *The LHCb Detector at the LHC*, J. Inst. **3**, S08005 (2008), doi:10.1088/1748-0221/3/08/S08005.

[2] R. Aaij et al., *LHCb detector performance*, Int. J. Mod. Phys. A **30**, 1530022 (2015), doi:10.1142/S0217751X15300227.

[3] R. Aaij et al., *Measurement of the nuclear modification factor and prompt charged particle production in pPb and pp collisions at $\sqrt{s_{NN}} = 5$ TeV* (2021), in preparation.

[4] S. Acharya et al., *Transverse momentum spectra and nuclear modification factors of charged particles in pp, p-Pb and Pb-Pb collisions at the LHC*, J. High Energy Phys. **11**, 013 (2018), doi:10.1007/JHEP11(2018)013.

[5] I. Helenius, K. J. Eskola and H. Paukkunen, *Probing the small-x nuclear gluon distributions with isolated photons at forward rapidities in p+Pb collisions at the LHC*, J. High Energy Phys. **09**, 138 (2014), doi:10.1007/JHEP09(2014)138.

[6] T. Lappi and H. Mäntysaari, *Single inclusive particle production at high energy from HERA data to proton-nucleus collisions*, Phys. Rev. D **88**, 114020 (2013), doi:10.1103/PhysRevD.88.114020.

[7] Z.-B. Kang, I. Vitev, E. Wang, H. Xing and C. Zhang, *Multiple scattering effects on heavy meson production in p+A collisions at backward rapidity*, Phys. Lett. B **740**, 23 (2015), doi:10.1016/j.physletb.2014.11.024.

[8] C. Aidala et al., *Nuclear-modification factor of charged hadrons at forward and backward rapidity in p+Al and p+Au collisions at $\sqrt{s_{NN}} = 200$ GeV*, Phys. Rev. C **101**, 034910 (2020), doi:10.1103/PhysRevC.101.034910.

[9] R. Aaij et al., *Measurement of prompt-cross-section ratio $\sigma(\chi_{c2})/\sigma(\chi_{c1})$ in pPb collisions at $\sqrt{s_{NN}} = 8.16$ TeV*, Phys. Rev. C **103**, 064905 (2021), doi:10.1103/PhysRevC.103.064905.

[10] R. Aaij et al., *Measurement of the relative rate of prompt χ_{c0}, χ_{c1} and χ_{c2} production at $\sqrt{s} = 7$ TeV*, J. High Energy Phys. **10**, 115 (2013), doi:10.1007/JHEP10(2013)115.

[11] R. Aaij et al., *Study of coherent J/ψ production in lead-lead collisions at $\sqrt{s_{NN}} = 5$ TeV* (2021), in preparation.

[12] K. Carvalho Akiba et al., *The HERSCHEL detector: high-rapidity shower counters for LHCb*, J. Inst. **13**, P04017 (2018), doi:10.1088/1748-0221/13/04/P04017.

[13] J. Adam et a., *Measurement of an Excess in the Yield of J/ψ at Very Low p_{T} in Pb–Pb Collisions at $\sqrt{s_{NN}} = 2.76$ TeV*, Phys. Rev. Lett. **116**, 222301 (2016), doi:10.1103/PhysRevLett.116.222301.

[14] J. Adam et al., *Observation of excess J/ψ yield at very low transverse momenta in Au+Au collisions at $\sqrt{s_{NN}} = 200$ GeV and U+U collisions at $\sqrt{s_{NN}} = 193$ GeV*, Phys. Rev. Lett. **123**, 132302 (2019), doi:10.1103/PhysRevLett.123.132302.

[15] E. Seifert and W. Cassing, *Baryon-antibaryon dynamics in relativistic heavy-ion collisions*, Phys. Rev. C **97**, 044907 (2018), doi:10.1103/PhysRevC.97.044907.